Chemical Science

ROYAL SOCIETY OF CHEMISTRY

EDGE ARTICLE

View Article Online
View Journal | View Issue

Cite this: *Chem. Sci.*, 2021, **12**, 4841

All publication charges for this article have been paid for by the Royal Society of Chemistry

Received 26th October 2020
Accepted 7th February 2021

DOI: 10.1039/d0sc05893a

rsc.li/chemical-science

Trioxatriangulenium ($TOTA^+$) as a robust carbon-based Lewis acid in frustrated Lewis pair chemistry†

Aslam C. Shaikh, José M. Veleta, Jules Moutet and Thomas L. Gianetti *

We report the reactivity between the water stable Lewis acidic trioxatriangulenium ion ($TOTA^+$) and a series of Lewis bases such as phosphines and N-heterocyclic carbene (NHC). The nature of the Lewis acid–base interaction was analyzed *via* variable temperature (VT) NMR spectroscopy, single-crystal X-ray diffraction, UV-visible spectroscopy, and DFT calculations. While small and strongly nucleophilic phosphines, such as PMe_3, led to the formation of a Lewis acid–base adduct, frustrated Lewis pairs (FLPs) were observed for sterically hindered bases such as $P(^tBu)_3$. The $TOTA^+$–$P(^tBu)_3$ FLP was characterized as an encounter complex, and found to promote the heterolytic cleavage of disulfide bonds, formaldehyde fixation, dehydrogenation of 1,4-cyclohexadiene, heterolytic cleavage of the C–Br bonds, and interception of Staudinger reaction intermediates. Moreover, $TOTA^+$ and NHC were found to first undergo single-electron transfer (SET) to form $[TOTA]\cdot[NHC]^{\cdot+}$, which was confirmed *via* electron paramagnetic resonance (EPR) spectroscopy, and subsequently form a $[TOTA–NHC]^+$ adduct or a mixture of products depending the reaction conditions used.

Introduction

Frustrated Lewis pairs (FLPs) arise from the combination of Lewis acids (LAs) and bases (LBs) with un-neutralized reactivity due to the steric repulsion between these units.[1] Since their discovery, FLPs have received considerable attention for their potential to activate small molecules and applications in catalysis in the absence of transition-metals.[2] While significant exploration of the tunability of FLPs has been done, it is interesting to note that the main advances are focused on the nature of the LBs. Common bases for FLPs found in the literature include a wide range of phosphines, amines, pyridines, N-heterocyclic carbenes (NHCs), or carbodiphosphoranes, which show compatibility with various solvents and functional groups during transformations. In contrast, the LA counterparts in FLPs are less versatile and mostly limited to perfluorinated alkyl/aryl boranes and alanes.[3] Group 13 molecules are often highly oxophilic which limits their use and stability in wet solvents, tolerance to several functional groups, and reaction conditions when applied in catalysis.[4] As a result, the development of versatile and stable LAs for FLP chemistry is still highly desirable.

In recent years, several cationic or electron-deficient compounds containing heavy elements of group 14 as LAs have been reported to show FLP reactivity, but their use remains underdeveloped.[5] Similarly, examples of Lewis acidic carbon centers in FLP chemistry are scarce,[6] and limited to trityl[4,7] and substituted trityl cations,[8] electron-deficient allenes,[9] *N*-methylacridinium salts,[10] cationic η^6-arene-Ru complex[11] and C_{60}-fullerenes[12] (Fig. 1a). However, similar to borane systems, most of these carbenium ions are air-sensitive, highly oxophilic, and experience side reactivity, which limit their applications. For example, trityl cation is an attractive LA due to its facile synthesis, but its negative pK_{R^+} of −6.7 makes it more oxophilic than most boron-based FLPs.[13] However, triaryl-carbenium ions are susceptible to a nucleophilic attack at the *para*-aryl, or *meta*-aryl positions, resulting in the formation of either cyclohexadienyl or aryl-phosphonium cations, which hampers the reactivity.[14] Heterocyclic fused carbenium analogues, such as acridinium, helicenium, and angulenium ions, are an attractive alternative.[15] Their more planar scaffold and reduced steric hindrance facilitates interaction at the central carbon. Furthermore, despite the increased stabilization and electron richness provided by the heteroatoms,[16] recent reports have shown that some of these carbocations retain a certain degree of Lewis acidity.[17]

Trioxatriangulenium ion ($TOTA^+$, Fig. 1b), first reported by Smith *et al.* in 1964 (ref. [18]) and with more recent applications in bioimaging and nucleic acid interaction,[19] is a planar heterocyclic fused carbenium ion with a pK_{R^+} of 9, a positive charge delocalized across the π-system, yet the central carbon contributing 33% of the LUMO's character, and with an acceptor number (AN) of 23.1.[20] As a result, $TOTA^+$ is water stable, resistant to *para*-aryl nucleophilic attack, and has shown preferential reactivities at the central carbon, with a variety of

University of Arizona, Department of Chemistry and Biochemistry, Tucson, AZ, USA. E-mail: tgianetti@arizona.edu

† Electronic supplementary information (ESI) available. CCDC 2035921–2035925. For ESI and crystallographic data in CIF or other electronic format see DOI: 10.1039/d0sc05893a

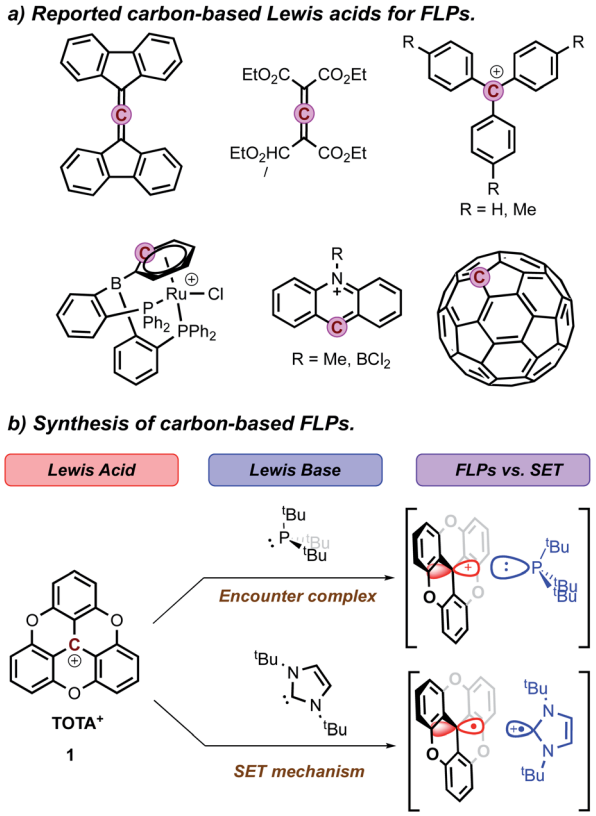

Fig. 1 (a) Previously reported carbon-based LA and (b) this work.

strong nucleophiles, such as hydride, sulfoxide, and organolithium or Grignard reagents, to form a cup-like molecule with an sp^3-hybridized central carbon, known as trioxatricornan.[21] While TOTA$^+$ is significantly less acidic than common Lewis acids such as $B(C_6F_5)_3$ (pK_a of 8.4 and AN of 80.1), the reported reactivity of TOTA$^+$ with small and hard nucleophiles,[22] led our group to investigate the nature of the interactions between TOTA$^+$ and softer LBs, such as phosphines.

Herein we describe the use of a trioxatriangulene (TOTA$^+$) as water stable LA for FLP chemistry, and its reactivity with different phosphines as LBs. The reactivity of the obtained FLPs was probed *via* the heterolytic disulfide bond cleavage, fixation of formaldehyde, C(sp^3)–H activation of 1,4-cyclohexadiene, heterolytic cleavage of a C–Br bond, and interception of Staudinger reaction intermediate. The interaction and reactivity of these FLPs are best described as encounter complexes. Furthermore, formation of Lewis acid–base adducts *via* single-electron transfer was observed between TOTA$^+$ and the N-heterocyclic carbene 1,3-di-*tert*-butylimidazol-2-ylidene (I^{t}Bu). The formation of these radical species is supported by UV-vis and EPR spectroscopies.

Results and discussion

A variety of alkyl, alkyl–aryl, and aryl phosphines were selected to probe the interaction between TOTA$^+$ and phosphines (Scheme 1a). Reacting the less sterical phosphine, PMe_3, with TOTA$^+$ resulted in the formation of a classical Lewis acid–base covalent adduct. This was observed by the instantaneous change in color upon the room temperature addition of PMe_3, changing from a dark yellow solution, characteristic of TOTA$^+$ (**1**) in CH_3CN, to a colorless solution. Such color change is consistent with the loss of conjugation in the π-system, due to a change in hybridization from sp^2 to sp^3 in the central carbon. The TOTA–$(PMe_3)^+$ adduct (**3a**) was isolated as a white solid in 96% yield (see Scheme 1 and ESI†). The ^{31}P NMR spectrum indicates the exclusive formation of a phosphonium species with a chemical shift of 39.7 ppm (Fig. S7†). The ^{1}H NMR spectrum of **3a** shows two sets of protons at $\delta = 7.53$ (td) and 7.12 (dd) ppm, consistent with the presence of a C_3 rotation axis, suggesting that the phosphorous is bound to the central carbon atom in TOTA. Slow CH_2Cl_2/hexane layering afforded colorless crystals of **3a** suitable for single-crystal X-ray diffractometry, that confirmed the formation of the covalent adduct at the central carbon (Scheme 1b and ESI†). The C1–P1 distance (1.864(1) Å) is comparable to typical C–P bonds (*ca.* 1.87 Å), yet shorter than the P–C bond in $[trityl\text{-}PMe_3]^+$ (1.887(4) Å)[14] and the P–B bond in tris(pentafluorophenyl)borane-phenylphosphane (2.039(4) Å).[23] These observations suggest that the planarity of the TOTA$^+$ scaffold promotes the formation of shorter bond in solid-state compared to the more sterically hindered trityl and borane structures. Within the asymmetric unit, the counter-anion BF_4^- is far from both the carbon and phosphorous centers in **3a** (B–C1 = 5.355 Å, B–P = 4.821 Å, or F–C1 = 4.573 Å and F–P = 3.891 Å respectively, see Fig. S110†).

Other phosphines with small cone angles, such as $PPhMe_2$, $P(^n Pr)_3$, and $P(^n Bu)_3$, also formed covalent Lewis adducts at room temperature, which were isolated in excellent yields (Scheme 1, **3a**, **3b**, **3c**, and **3d**, respectively).[24] Interestingly, when the TOTA–$P(^n Bu)_3^+$ adduct (**3d**) was warmed up to 353 K in CD_3CN, a broadening of the ^{1}H NMR resonances are observed (Fig. S19†), suggesting the presence of a thermodynamic equilibrium. Using PPh_2Me, a phosphine of similar cone angle as $P(^n Bu)_3$ yet with lower basicity, broad and unresolved peaks in the ^{1}H NMR spectrum were observed at room temperature, suggesting that the slow exchange regime of the equilibrium is observable on the NMR time scale at room temperature (Scheme 1a, **3e**). Variable temperature ^{1}H NMR analysis, along with the thermochromic change of the solution, confirmed the presence of a reversible adduct in which the Lewis adduct is the major species at low temperatures (see Fig. 2 and ESI†).

Continuing with the trend, when TOTA$^+$ was mixed with a weakly basic phosphine such as PPh_3 (Scheme 1a, **3f**), or a sterically hindered phosphines, such as $P(^t Bu)_3$ (Scheme 1a, **3g**), no Lewis adduct was observed by NMR spectroscopy at either room or low temperatures. Neither the appearance of a new peak in ^{31}P NMR spectroscopy nor an upfield shift of the aromatic region in TOTA$^+$ protons, characteristic of the trioxatricornan scaffold, was observed (see ESI†). However, we noted that, in both CD_2Cl_2 or CD_3CN solvents, the aromatic resonances of TOTA$^+$ appear as broad signals at room temperature, and sharpened at lower temperatures (Fig. S27–S30 and S36–S40†). Furthermore, when lowering the temperature below 230 K, a broadening of the *tert*-butyl and phenyl signals were

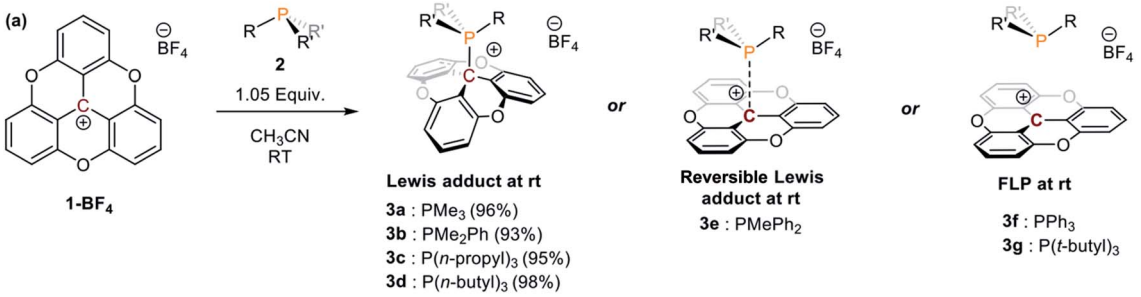

(b)

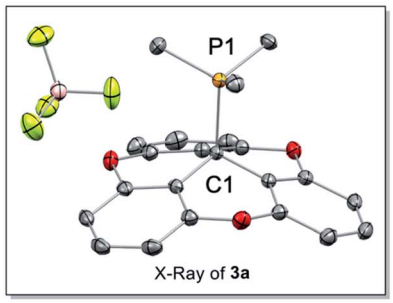

(c)

Type of Interaction	Phosphine	Cone angle (°)	Basicity (pK_A)[44]	Calculated ΔH_{adduct} (kcal.mol^{-1})
Lewis adduct at rt	**2a**, PMe_3	118	8.7	-23.44
	2b, $PPhMe_2$	122	6.5	-26.24
	2c, P(*n*- propyl)$_3$	132	8.6	-32.74
	2d, P(*n*-butyl)$_3$	136	8.3	-22.74
Reversible adduct at rt	**2e**, PPh_2Me	136	4.6	-16.50
FLP at rt	**2f**, PPh_3	145	2.7	-12.87
	2g, P(*t*-butyl)$_3$	182	11.7	-11.84

Scheme 1 (a) Reactivity of phosphines (**2a–2g**) towards TOTA$^+$. (b) ORTEP of the X-ray structure of **3a**. Hydrogen atoms and counter ion are omitted for clarity. (c) Summary of cone angle, Lewis basicity, and DFT calculated ΔH_{adduct} (enthalpy of adduct formation relative to free TOTA and phosphine) for phosphines **2a–2g**.

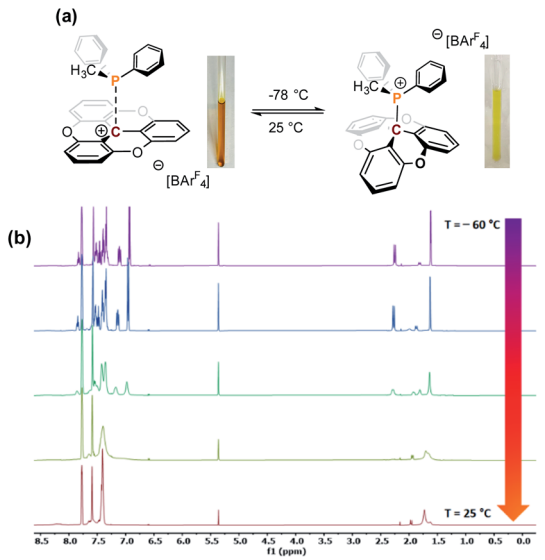

Fig. 2 (a) Reversible Lewis adduct formation between TOTA$^+$ and PPh_2Me. (b) Variable temperature (VT) 500 MHz ^{1}H NMR spectra of TOTA$^+$ (12 mg, 0.01 mmol) and PPh_2Me (4.2 mg, 0.02 mmol) in CD_2Cl_2 indicating formation Lewis adduct at −60 °C.

observed in the ^{1}H NMR spectra (Fig. S27 and S37†). The broadening and coalescences of the TOTA$^+$ aromatic peaks and the phosphine substituents indicate that only a weak van der Waals adduct is formed, as observed in the case of FLPs derived from $B(C_6F_5)_3$ and bulky phosphines, and that these aggregates have random relative orientations (see DFT calculations *vide infra*).[8,25] Diffusion ordered spectroscopy (DOSY) NMR experiments were performed and further supported the formation of such aggregates (see ESI, Fig. S31–S34 and S41 and S42†).[26] For example, the diffusion coefficients (D) for **1-BAr$^F_4$** and P(^{t}Bu$_3$) alone are 1.41 × 10^{-9} m^2 s^{-1} and 1.88 × 10^{-9} m^2 s^{-1} respectively. However, upon mixing, diffusion coefficients of 1.80 × 10^{-9} m^2 s^{-1} (**1-BAr$^F_4$**) and 1.74 × 10^{-9} m^2 s^{-1} (P(^{t}Bu$_3$)) were recorded.[27] Finally, we noted that upon mixing TOTA$^+$ and P(^{t}Bu)$_3$ a slightly darker yellow color, compared to that of TOTA$^+$, was observed. This was further analyzed by mixing an equimolar amounts of each species in CH_2Cl_2 and analyzing the solution *via* UV-vis absorption spectroscopy. We observed the appearance of weak absorption bands at λ_{max} of 576 and 626 nm, in addition to the main absorption bands for TOTA$^+$

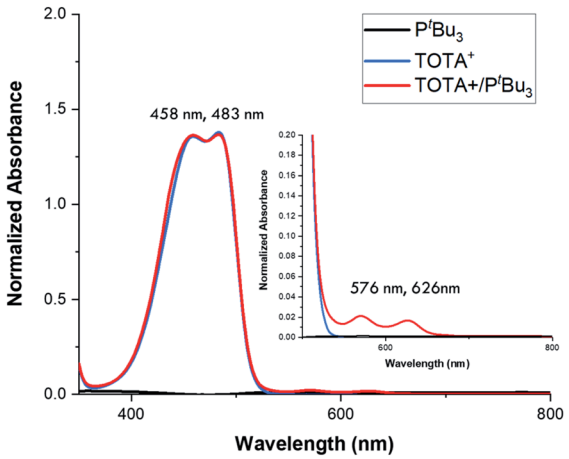

Fig. 3 Normalized UV-vis spectra of TOTA$^+$ (blue trace, 1 × 10^{-5} M in CH_2Cl_2), P^{t}Bu$_3$ (black trace, 1 × 10^{-5} M in CH_2Cl_2), and a 1 : 1 mixture of P^{t}Bu$_3$/TOTA$^+$ (red trace, both substrates 1 × 10^{-5} M in CH_2Cl_2).

(458 and 483 nm) (see Fig. 3). These data indicate the presence of an encounter complex in solution.[28] We postulate that the increased steric bulk of the phosphine inhibits the formation of a Lewis adduct, resulting in a dynamic equilibrium between free $TOTA^+/P(^tBu)_3$ and its encounter complex.

Density functional theory (DFT) calculations were used to further understand the energetic and steric factors between $TOTA^+$ and the different phosphines (Scheme 1c and ESI†). As expected, the strength of the LA–LB interaction, quantified *via* both the $[P–C_{TOTA}]^+$ bond length and stabilization energy, depends on the phosphine's cone angle and basicity. For example, the $TOTA^+$-adducts with phosphines of comparable LB character, such as PMe_3, $P(^nBu)_3$, and $P(^tBu)_3$, show a correlation between increasing cone angle and increasing $[P–C_{TOTA}]^+$ bond length. The $[TOTA–PMe_3]^+$ adduct had the shortest bond compared to the $[TOTA–P(^tBu)_3]^+$ (1.88 *vs.* 2.06 Å, Table S11†). Similarly, the stabilization energy for these adducts was inversely proportional to the cone angle of the phosphine used, with decreasing energies of −23.4, −16.5, and −11.8 kcal mol^{-1} for increasing cone angles (Me < ^{n}Bu < ^{t}Bu, see ESI†). Looking at phosphines with comparable cone angles, such as PPh_2Me and $P(^nBu)_3$ (cone angle of 136°), a shorter $[P–C_{TOTA}]^+$ bond length by 0.02 Å and larger stabilization energy (−22.7 *vs.* −16.5 kcal mol^{-1}) was observed for the more Lewis basic $P(^nBu)_3$.

DFT calculations also provided insight on the structure of the FLPs aggregates. For both FLPs, several conformers of close energy were found (see ESI† and Fig. 4), with the most thermodynamic stable aggregate, **3f-I** and **3g-I**, being more favorable than the free components by ∼12 kcal mol^{-1} (see Fig. 5). For $[TOTA–PPh_3]^+$, the most thermodynamically stable conformer **3f-I** contains a π–π stacking interaction between the planar $TOTA^+$ and the arylphosphine, where the phosphorus atom is pointing away from the carbocation scaffold, while **3f-II** shows a P–C interaction characteristic of a Lewis adduct (Fig. 4a). With $[TOTA–P(^tBu)_3]^+$, the thermodynamically favorable conformation **3g-I** has the phosphorus atom directly in front of central carbon atom of $TOTA^+$, while in **3g-II** the P atom is pointing in the opposite direction (Fig. 4b). These calculations support the NMR spectra obtained for these FLPs (*vide supra*).

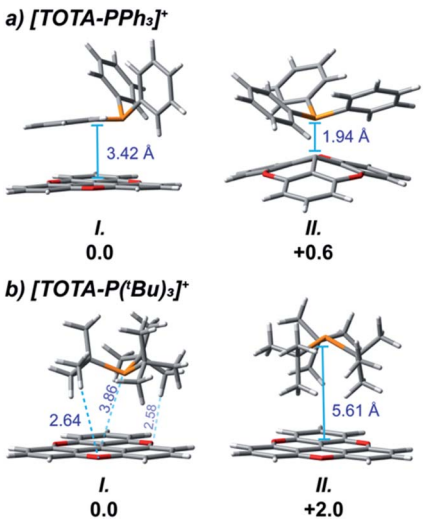

Fig. 4 DFT geometry optimized structures of $TOTA^+$ adducts with (a) PPh_3 and (b) $P(^tBu)_3$ using the CAM-B3LYP functional and 6-311G(d,p) basis set with PCM for acetonitrile (relative energy in kcal mol^{-1}).

We then tested the reactivity of our Lewis pairs for the activation of non-polar covalent bonds, such as those present in disulfides. Using diphenyl sulfide, we observed full conversion in good yields for the desired S–S bond cleavage products at room temperature for the FLP encounter complexes **3f** and **3g**.

In the case of the reaction with **3g**, the initially dark yellow solution gradually turned colorless after 10 min at room temperature. The crude mixture was thoroughly washed with pentane, and crystallization at −20 °C of the pentane washes resulted in TOTA–SPh (**4a**) as colorless crystals. The formation of **4a** was supported by the conservation of the C_3 rotation axis and two set of protons for the $TOTA^+$ moieties in the ^{1}H NMR spectrum, as well as the presence of a new quaternary carbon signal at 40.9 ppm in the $^{13}C\{^1H\}$ NMR spectrum. Furthermore, the structure of **4a** was unambiguously confirmed by X-ray diffraction crystallography which attests to the heteroleptic cleavage of the disulfide bond of $(SPh)_2$ (Scheme 2b). Notably, the C1–S1 bond of 1.902(2) Å is slightly longer than the typical value for single C–S bond length (∼1.83 Å), but is consistent with the covalent C–S distance found in the sulfide(trityl) bond (C–S = 1.90 Å).[29] Moreover, the solid residue from the washes was dried under vacuum for 12 h, and the yellow compound was crystallized from slow diffusion of pentane into a concentrated solution in CH_2Cl_2 at −20 °C. The desired thio-phosphonium salt (**5a**) was isolated in pure form and characterized by NMR spectroscopy (Scheme 2a and ESI†). We further tested the ability of **3g** to cleave the S–S bond of a variety of disulfides RS–SR (R = *p*-tolyl, 4-Cl-C_6H_4, –Bn) which gave the desired products **4b–4d** and **5b–5d** in good yields. Similar reactivity was observed when the FLP-**3f** was used. The desired S–S bond cleavage products were isolated in excellent yields (Scheme 2a and see ESI†).

It is noted that $TOTA^+$ or phosphine alone were inert towards the disulfide bond cleavage (Scheme 2b). Excitingly, when the disulfide cleavage was performed in wet acetonitrile, the desired products were obtained in high yields (Scheme 2b). This result highlights the robustness and water tolerance of the system. Interestingly, the covalent adducts **3a** and **3d** also resulted in S–S bond cleavage but required temperatures of 60 °C and 35 °C respectively (see Scheme 2b and ESI†). Furthermore, premixing the PMe_3 with disulfide, followed by addition of $TOTA^+$, resulted in a mixture of the desired S–S bond cleavage product along with TOTA–PMe_3 adduct **3a**. These observations suggest that LA–LB dissociation is needed to promote disulfide activation.[30]

The reaction coordinate for the activation of disulfide bonds was studied using DFT (Fig. 5). Grimme D3 empirical dispersion damping forces were applied to better understand non-covalent interactions between the $TOTA^+$, $(SPh)_2$, and PR_3 (R = Me, Ph, ^{t}Bu) fragments. Starting from the FLP or covalent adduct (step 1, Fig. 5), a dissociation step in the presence of $(SPh)_2$ is considered (step 2, Fig. 5). As observed experimentally, the dissociation energies for the $TOTA^+$ adducts with PPh_3 and $P(^tBu)_3$ is

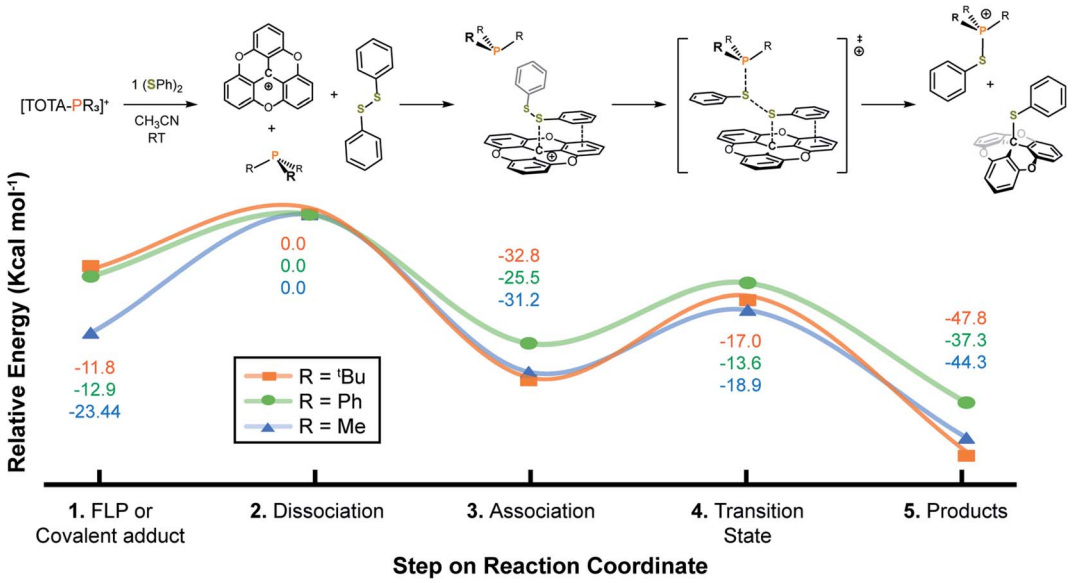

Fig. 5 Reaction coordinate for the activation of $(SPh)_2$ using $[TOTA–PR_3]^+$ (R = ^{t}Bu, Ph, or Me) adducts. All models were calculated using the CAM-B3LYP functional, 6-311G(d,p) basis set, SCRF PCM acetonitrile solvation model, and Grimme D3 empirical dispersion damping functions. Transition states were found with a single imaginary frequency and as local maxima by IRC calculations.

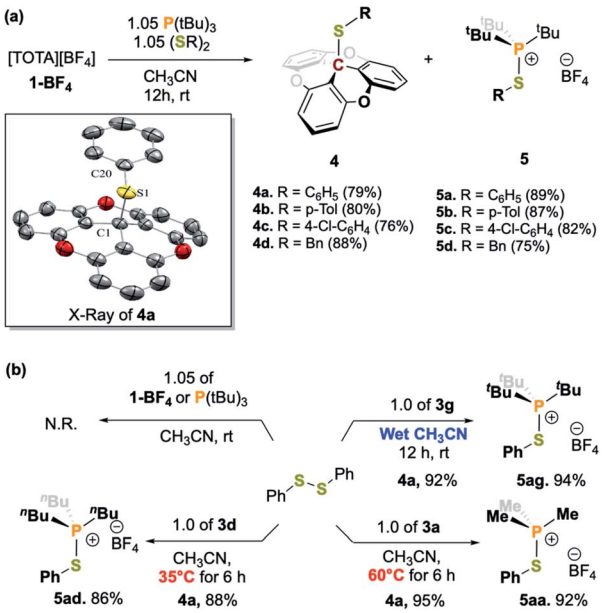

Scheme 2 (a) FLP-mediated activation of disulfide bonds and crystal structures of **4a** (thermal ellipsoids shown at 50% probability, hydrogen atoms and counter ions are omitted for clarity. C grey, O red, S yellow). (b) Control experiments, Lewis adduct mediated S–S bond cleavage with **3a** and **3d**, as well as **3g** in wet solvent.

thermodynamically more accessible than for PMe_3, with a dissociation barrier ducts *ca.* 10 kcal mol^{-1} more accessible for PPh_3 and $P(^tBu)_3$ than for the PMe_3 adduct. In the following step, a TOTA–SPh intermediate stabilized by π-stacking interactions between the aryl groups in TOTA and the disulfide substrate is formed (step 3, Fig. 5). The π-complex is then attacked by the phosphine *via* a concerted transition state (step 4, Fig. 5). The overall reaction coordinate for the activation of $(SPh)_2$ is representative of an exothermic process, with the formation of TOTA–SPh and $[R_3P–SPh]^+$ adducts *ca.* 40 kcal mol^{-1} lower in energy than the correspondent reactants (FLP or adducts, step 5, Fig. 5).

We further examined the utility of the FLP **3g** towards bond activation using 1,4 cyclohexadiene,[7a] and ^{t}butyl bromide (Scheme 3). Addition of 1,4-cyclohexadiene to a solution of **3g** in acetonitrile resulted in the dehydrogenation of hexadiene to form benzene, the formation of the phosphonium salt **7** in 86% yield and trioxatricornan TOTA–H (**6**) in 64% yield. The phosphonium salt shows a characteristic P–H signal at 6.25 ppm in the ^{1}H NMR spectrum and a doublet at 50.52 ppm in the ^{31}P NMR spectrum, with a $^1J_{P–H}$ coupling constant of 469.8 Hz (see ESI†). The reactivity of **3g** towards ^{t}butyl bromide resulted in the formation of phosphonium salt **7** and [TOTA][Br] in quantitative yields, with the expected isobutylene side-product as reported by Wass *et al.*[31] Importantly, no reaction was observed upon exposure of **3g** to H_2 gas, at either atmospheric pressure or 4 bar, with or without saturated substrates such as alkyne.

Next, we investigated the reactivity of FLP **3g** toward unsaturated substrates such as formaldehyde and benzyl azide (Scheme 3). When a 1.0 molar equivalent of paraformaldehyde was added to a solution of **3g**–BF_4 in CH_3CN, we observed the formation of a new product by NMR spectroscopy, assigned to a formaldehyde adduct. However, the new species slowly returns to the starting material suggesting that the strongly coordinating acetonitrile was not suited to isolate the adduct formed. To improve the stability of the adduct formed we turned to the non-coordinating solvent CH_2Cl_2. Since [TOTA][BF_4] is sparingly soluble in this solvent, we synthesized the more soluble [TOTA][$BAr^F{}_4$] analog ($[BAr^F{}_4]^-$ = $[\{3,5\text{-}(CF_3)_2\text{-}C_6H_3\}_4B]^-$) following previously reported literature.[17a] An

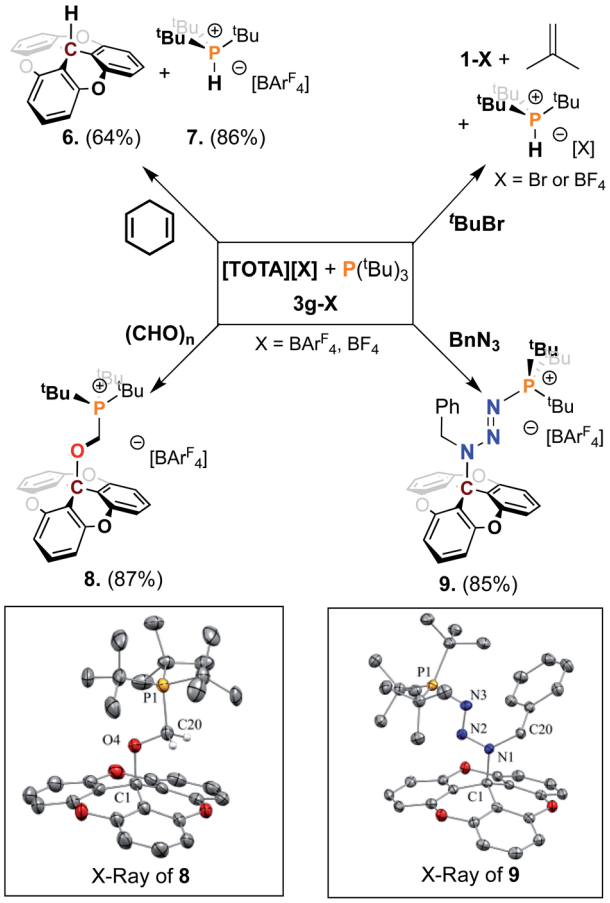

Scheme 3 FLPs mediated activation of small molecules. Unless otherwise noted all reactions were carried out on a 0.05 mmol scale using [**1**$^+$], 0.05 mmol P(^{t}Bu)$_3$, 4 ml solvent, at room temperature. Isolated yields are given in parentheses (BAr^F_4 = tetrakis(3,5-bis(trifluoromethyl)phenyl)borate). Crystal structures of **8** and **9**; (thermal ellipsoids shown at 50% probability, hydrogen atoms and counter ion are omitted for clarity. P orange, N blue, C grey, O red).

equimolar solution of **3g**–BAr^F_4 and paraformaldehyde were stirred for 24 h at room temperature in CH_2Cl_2. The resultant colorless turbid solution was dried under vacuum, and the residue was washed with pentane affording the formaldehyde adduct **8**. Slow diffusion of pentane into a CH_2Cl_2 concentrated solution at −20 °C led to the formation of colorless single crystals of **8**. Analysis *via* ^{31}P and ^{1}H NMR spectroscopies revealed the presence of resonances that support the complexation of formaldehyde in between the FLP **3g** ($\delta_{^{31}P}$ = 44.2 ppm, $\delta_{^{13}C}$ = 50.27 (d, J = 55.5 Hz), and $\delta_{^1H}$ = 4.63 ppm (d, J = 5.4 Hz, CH_2)). The structure of **8** was unambiguously confirmed by single crystal X-ray diffraction (Scheme 3), showing the formation of a single bond between the carbon center of TOTA and the oxygen of paraformaldehyde with a C1–O4 of 1.513(4), longer than a classic C–O bond (*ca.* 1.43 Å). The C20–P1 bond length of 1.825(4) Å is consistent with a single carbon–phosphorus bond. We also noted that the elongated C20–O4 bond (1.410(5) Å *vs.* 1.2 Å in classic C=O bond) support a single bond and the reduction of the paraformaldehyde to an alcoholate (see ESI†).

Finally, an organic azide was employed which led to the isolation of a Staudinger-type reaction intermediate from the reaction between P(^{t}Bu)$_3$, TOTA$^+$, and benzyl azide. The combination of **3g** and benzyl azide in CH_2Cl_2 afforded adduct **9** in 85% yield after 12 h at room temperature (Scheme 3). NMR and crystallographic analysis of **9** revealed it to be the addition product of BnN_3 between TOTA$^+$ and P(^{t}Bu)$_3$ (Scheme 3). Suitable crystals for X-ray diffraction studies of **9** were obtained by slow diffusion of pentane into a concentrated CH_2Cl_2 solution, resulting in pale-yellow plates. The trapping of Staudinger-type intermediate by **3g** is characterized by the creation of a single C1–N1 bond (benzyl nitrogen from the substrate) length of 1.524(4) Å longer than the classic C–N bond (~1.47 Å). At the same time, an N3–P1 bond is formed with the terminal nitrogen (1.680(3) Å) and the P(^{t}Bu)$_3$ having a typical length of a phosphorus–azide bond (1.658(3) Å).[27] It was further noted that the distances N1–N2 and N2–N3 (respectively 1.310(3) and 1.299(3) Å) retain a double bond character while the length of the N1–C20 bond (1.467(3) Å) of the benzyl group is also unaffected. This FLP addition reaction is consistent and can be compared to literature examples for a range of aryl azides and trityl-boron or phosphorous–boron FLPs.[7a,27,32]

To test the compatibility of TOTA$^+$ with other Lewis bases, we used an NHC, 1,3-di-*tert*-butylimidazol-2-ylidene (I^{t}Bu, **10**), as a possible LB (see Scheme 4 and Table S2†). Upon addition of **10** to a solution of [TOTA][BAr^F_4] in toluene at room temperature, an immediate light green solution was observed which quickly turned to pale yellow. Analysis *via* ^{1}H NMR spectroscopy of the crude reaction mixture shows the formation of C4-adduct (**11**, 79%), and C2-adduct (**11′**, 10%), and a minor byproduct assigned to the imidazole salt (**12**, 10%). When the reaction was performed at −78 °C, the C4/C2 selectivity was reversed, and the

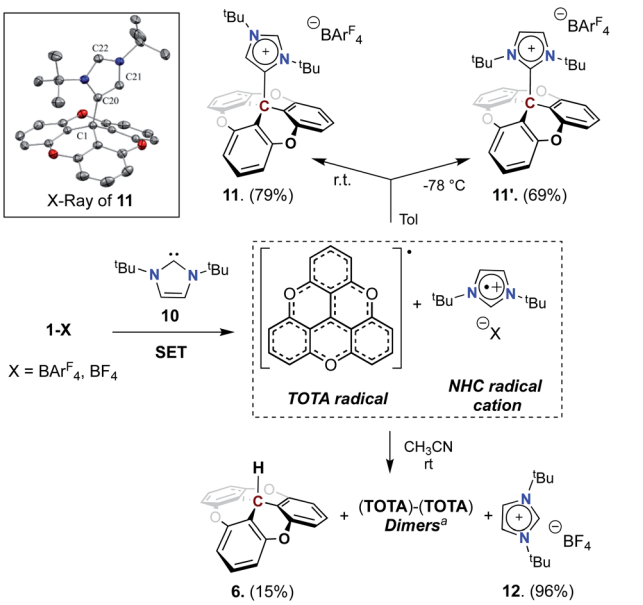

Scheme 4 Reactivity of TOTA$^+$ with NHC carbene. [a]Unless otherwise noted all reactions were carried out on a 0.05 mmol scale using [**1**$^+$], 0.05 mmol I^{t}Bu (**10**), 4 ml solvent, rt. [a]See ESI† for dimer structures.

predominant formation of the C2 adduct **11′** was observed, along with a trace of imidazole salt. The two isomers are easily differentiated by ^{1}H NMR spectroscopy, specifically with the signals corresponding to the ^{t}Bu groups. In the C4-adduct **11**, the ^{t}Bu groups are non-equivalent (1.36 and 1.34 ppm), while the C2-adduct **11′** conserves a C_2 rotation axis rendering both ^{t}Bu groups equivalent (1.53 ppm). Furthermore, crystals of **11**, obtained by slow diffusion of pentane into CH_2Cl_2 at −20 °C, were subjected to X-ray diffraction analysis which confirmed its structure as a C4–NHC adduct (Scheme 4). As observed in NMR, the formation of the thermodynamically favorable compound ("C4" adduct) is characterized by the formation of the single bond C1–C20 (1.565(3) Å) corresponds to the homolytic coupling product following the SET process. This bond, although slightly longer than a standard C–C ((∼1.54) Å, +0.02 Å) has a covalent character that is only weakened by the steric hindrance imposed by the ^{t}Bu groups. The presence of a C=C double bond is also noted between the C20–C21 atoms (1.361(3) Å) as postulated by ^{1}H NMR spectroscopy.

Interestingly, when $TOTA^+$ and I^{t}Bu were mixed in CH_3CN at room temperature a deep-green solution was formed, which immediately turned to brown with a purple precipitate. From the reaction mixture, the imidazolium salt (**12**), TOTA–H (**7**), TOTA-dimers were isolated, with only traces of the C4-adduct (**11**) (see Scheme 4 and ESI†). The TOTA-dimers formation can be rationalized by the dimerization of $TOTA^{\cdot}$ radicals.[33] However, consistent with previous report of such radical,[34] monitoring the CH_3CN reaction mixture by UV-Vis spectroscopy and EPR spectroscopy did not allow the observation of $TOTA^{\cdot}$ radical (see Fig. S107†).[35] Trapping experiments with TEMPO and benzoyl peroxide were also unsuccessful (see ESI†). These observations suggest that a single electron transfer (SET)[36] between $TOTA^+$ and the NHC occurred, and then followed by radical recombination to form **11** or **11′** in non-polar solvent such as toluene, or a mixture of products in dissociative solvent such as acetonitrile. The calculated electron affinity and ionization potential of $TOTA^+$ (−7.41 eV) and I^{t}Bu (+5.59 eV) suggest that SET process in the ground state is accessible (see Table S15†).[37]

The TOTA–NHC adducts **11** and **11′** were studied using computational methods (Fig. 6). As observed experimentally, the ground state configuration of the adduct corresponds to **11** (C4–NHC adduct); being lower in energy than its conformational isomer **11′** by 37.8 kcal mol^{-1}. The difference in energy is also reflected in the elongation of the $C_{(TOTA)}$–$C_{(NHC)}$ bond distances, with a 0.06 Å difference between the C4 and C2 adduct. These differences in energy and bond distances are attributed to the increased steric hindrance of the C2 adduct, where both ^{t}Bu groups are in close proximity to TOTA, compared to the C4 adduct, where one of the ^{t}Bu groups is pointing away of TOTA.

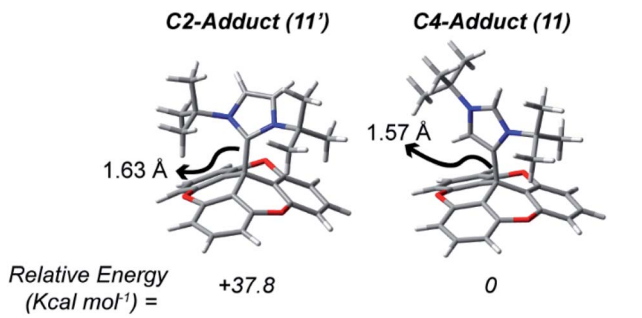

Fig. 6 Relative energy and bond TOTA–NHC bond distances from the calculated DFT models of **11** and **11′**.

Conclusions

We have demonstrated that trioxatrianguleniums ($TOTA^+$) and sterically hindered phosphines, such as P(^{t}Bu)$_3$, can act as a frustrated Lewis pair. The VT-NMR experiments, single crystal X-ray diffraction crystallography, and UV-visible spectroscopic analysis supports the existence of a FLP encounter complex. These newly identified FLPs mimic the reactivity of main group FLPs in reactions such as heterolytic S–S bond cleavage, dehydrogenation of 1,4-cyclohexadiene, fixation of formaldehyde, C–Br bond cleavage in *tert*-butyl bromide, and interception of a Staudinger reaction intermediate. DFT calculations have demonstrated the possible reactivity mode of the FLP system for disulfide cleavage. Furthermore, the reactivity of $TOTA^+$ with other Lewis bases such as NHC was investigated. Control experiments and EPR studies revealed that this pair undergoes the SET step for the formation Lewis acid–base adduct. It is noteworthy that this carbon-based Lewis acid is significantly less oxophilic than boron, aluminum, and silicon-based Lewis acids, making it both air and moisture stable. Considering the efficiency of this FLPs system, it could be useful for other organic transformation in the future. Extending this family of carbon Lewis acids by developing FLPs containing other trioxatrianguleniums salts with and different Lewis bases are ongoing in our lab.

Conflicts of interest

There are no conflicts to declare.

Acknowledgements

We are grateful for financial support from the University of Arizona for this work. We thank Dr Andrei Astashkin (EPR and X-Ray facility of the University of Arizona) for performing the EPR measurements and helping with the analysis of the EPR spectra, as well as providing help for the XRD data collection and analysis. All NMR data were collected in the NMR facility of the Department of Chemistry and Biochemistry at the University of Arizona, and we thank Dr Jixun Dai for his help with 2D-NMR analysis. The purchase of the Bruker NEO 500 MHz spectrometer were supported by the National Science Foundation under Grant Number 1920234, and the University of Arizona. J. M. V. thanks the diversity and inclusion efforts from individuals, groups, and institutions towards a more united science community.

Notes and references

1 (*a*) D. W. Stephan and G. Erker, *Angew. Chem. Int. Ed.*, 2015, **54**, 6400–6441; *Angew. Chem.*, 2015, **127**, 6498–6541; (*b*) D. W. Stephan, *J. Am. Chem. Soc.*, 2015, **137**, 10018–10032; (*c*) G. Erker and D. W. Stephan, *Frustrated Lewis Pairs I: Uncovering and Understanding*, Springer, New York, 2013; (*d*) G. Erker and D. W. Stephan, *Frustrated Lewis Pairs II: Expanding the Scope*, Springer, New York, 2013; (*e*) J. S. J. McCahill, G. C. Welch and D. W. Stephan, *Angew. Chem. Int. Ed.*, 2007, **46**, 4968–4971; *Angew. Chem.*, 2007, **119**, 5056–5059.

2 (*a*) L. Liu, B. Lukose, P. Jaque and B. Ensing, *Green Energy Environ.*, 2019, **4**, 20–28; (*b*) S. Mukherjee and P. Thilagar, *J. Chem. Sci.*, 2015, **127**, 241–255; (*c*) D. W. Stephan, *Acc. Chem. Res.*, 2015, **48**, 306–316; (*d*) D. W. Stephan, *Org. Biomol. Chem.*, 2008, **6**, 1535–1539.

3 (*a*) L. C. Wilkins and R. L. Melen, *Encycl. Inorg. Bioinorg. Chem.*, 2017, **1**, 1–24; (*b*) D. W. Stephan, *Science*, 2016, **354**, aaf7229.

4 S. A. Weicker and D. W. Stephan, *Bull. Chem. Soc. Jpn.*, 2015, **88**, 1003–1016.

5 (*a*) T. A. Kinder, R. Pior, S. Blomeyer, B. Neumann, H. G. Stammler and N. W. Mitzel, *Chem.–Eur. J.*, 2019, **25**, 5899–5903; (*b*) D. J. Scott, N. A. Phillips, J. S. Sapsford, A. C. Deacy, M. J. Fuchter and A. E. Ashley, *Angew. Chem., Int. Ed.*, 2016, **55**, 14738–14742; *Angew. Chem.*, 2016, **128**, 14958–14962; (*c*) T. J. Herrington, B. J. Ward, L. R. Doyle, J. McDermott, A. J. P. White, P. A. Hunt and A. E. Ashley, *Chem. Commun.*, 2014, **50**, 12753–12756; (*d*) M. Reißmann, A. Schäfer, S. Jung and T. Müller, *Organometallics*, 2013, **32**, 6736–6744.

6 M. Alcarazo, *Dalton Trans.*, 2011, **40**, 1839–1845.

7 (*a*) J. Zhou, L. L. Cao, L. Liu and D. W. Stephan, *Dalton Trans.*, 2017, **46**, 9334–9338; (*b*) M. H. Holthausen, T. Mahdi, C. Schlepphorst, L. J. Hounjet, J. J. Weigand and D. W. Stephan, *Chem. Commun.*, 2014, **50**, 10038–10040; (*c*) J. W. Runyon, O. Steinhof, H. V. R. Dias, J. C. Calabrese, W. J. Marshall and A. J. Arduengo III, *Aust. J. Chem.*, 2011, **64**, 1165–1172; (*d*) P. A. Chase, A. L. Gille, T. M. Gilbert and D. W. Stephan, *Dalton Trans.*, 2009, 7179–7188.

8 E. Follet, P. Mayer, D. S. Stephenson, A. R. Ofial and G. Berionni, *Chem.–Eur. J.*, 2017, **23**, 7422–7427.

9 (*a*) D. Palomas, S. Holle, B. Inés, H. Bruns, R. Goddard and M. Alcarazo, *Dalton Trans.*, 2012, **41**, 9073–9082; (*b*) B. Inés, D. Palomas, S. Holle, S. Steinberg, J. A. Nicasio and M. Alcarazo, *Angew. Chem., Int. Ed.*, 2012, **51**, 12367–12369; *Angew. Chem.*, 2012, **124**, 12533–12536; (*c*) B. Inés, S. Holle, R. Goddard and M. Alcarazo, *Angew. Chem., Int. Ed.*, 2010, **49**, 8389–8391; *Angew. Chem.*, 2010, **122**, 8567–8569.

10 (*a*) E. J. Lawrence, E. R. Clark, L. D. Curless, J. M. Courtney, R. J. Blagg, M. J. Ingleson and G. G. Wildgoose, *Chem. Sci.*, 2016, **7**, 2537–2543; (*b*) E. R. Clark and M. J. Ingleson, *Angew. Chem., Int. Ed.*, 2014, **53**, 11306–11309; *Angew. Chem.*, 2014, **126**, 11488–11491; (*c*) E. R. Clark and M. J. Ingleson, *Organometallics*, 2013, **32**, 6712–6717.

11 M. P. Boone and D. W. Stephan, *J. Am. Chem. Soc.*, 2013, **135**, 8508–8511.

12 (*a*) J. Iglesias-Sigüenza and M. Alcarazo, *Angew. Chem., Int. Ed.*, 2012, **51**, 1523–1524; *Angew. Chem.*, 2012, **124**, 1553–1555; (*b*) H. Li, C. Risko, J. H. Seo, C. Campbell, G. Wu, J. L. Brédas and G. C. Bazan, *J. Am. Chem. Soc.*, 2011, **133**, 12410–12413.

13 V. R. Naidu, S. Ni and J. Franzén, *ChemCatChem*, 2015, **7**, 1896–1905.

14 (*a*) J. Bosson, G. M. Labrador, C. Besnard, D. Jacquemin and J. Lacour, *Angew. Chem., Int. Ed.*, 2021, DOI: 10.1002/anie.202016643; (*b*) A. C. Shaikh, J. M. Veleta, J. Bloch, H. J. Goodman and T. L. Gianetti, *Eur. J. Org. Chem.*, 2020, **17**, 2553–2559; (*c*) K. Chansaenpak, M. Yang and F. P. Gabbaï, *Philos. Trans. R. Soc. London, Ser. A*, 2017, **375**, 2017000; (*d*) R. Vanel, F.-A. Miannay, E. Vauthey and J. Lacour, *Chem. Commun.*, 2014, **50**, 12169–12172; (*e*) L. Cabrera, G. C. Welch, J. D. Masuda, P. Wei and D. W. Stephan, *Inorg. Chim. Acta*, 2006, **359**, 3066–3071.

15 J. Bosson, J. Gouin and J. Lacour, *Chem. Soc. Rev.*, 2014, **43**, 2824–2840.

16 (*a*) M. Marinova, S. Pascal, L. Guénée, C. Besnard, B. Shivachev, K. Kostova, C. Villani, R. Franzini, V. Dimitrov and J. Lacour, *J. Org. Chem.*, 2020, **85**, 11908–11923; (*b*) I. H. Delgado, S. Pascal, C. Besnard, S. Voci, L. Bouffier, N. Sojic and J. Lacour, *Chem.–Eur. J.*, 2018, **24**, 10186–10195; (*c*) I. Hernandez Delgado, S. Pascal, A. Wallabregue, R. Duwald, C. Besnard, L. Guénée, C. Nançoz, E. Vauthey, R. C. Tovar, J. L. Lunkley, G. Muller and J. Lacour, *Chem. Sci.*, 2016, **7**, 4685–4693.

17 (*a*) W.-C. Liu, Y. Kim and F. P. Gabbai, *Chem.–Eur. J.*, 2021, DOI: 10.1002/chem.202100389; (*b*) G. Park and F. P. Gabbaï, *Chem. Sci.*, 2020, **11**, 10107–10112; (*c*) A. C. Shaikh, J. Moutet, J. M. Veleta, M. Hossain, J. Bloch, A. V. Astashkin and T. L. Gianetti, *Chem. Sci.*, 2020, **11**, 11060–11067; (*d*) L. Mei, J. M. Veleta, J. Bloch, H. J. Goodman, D. Pierce-Navarro, A. Villalobos and T. L. Gianetti, *Dalton Trans.*, 2020, **49**, 16095–16105; (*e*) M. Karimi, R. Borthakur, C. L. Dorsey, C.-H. Chen, S. Lajeune and F. P. Gabbaï, *J. Am. Chem. Soc.*, 2020, **142**, 13651–13656; (*f*) L. Wilkins, Y. Kim, E. Litle and F. P. Gabbaï, *Angew. Chem., Int. Ed.*, 2019, **58**, 18266–18270; *Angew. Chem.*, 2019, **131**, 18434–18438.

18 J. C. Martin and R. G. Smith, *J. Am. Chem. Soc.*, 1964, **86**, 2252–2256.

19 (*a*) B. Qiao, B. E. Hirsch, S. Lee, M. Pink, C.-H. Chen, B. W. Laursen and A. H. Flood, *J. Am. Chem. Soc.*, 2017, **139**, 6226–6233; (*b*) A. Shivalingam, A. Vyšniauskas, T. Albrecht, A. J. P. White, M. K. Kuimova and R. Vilar, *Chem.–Eur. J.*, 2016, **22**, 4129–4139; (*c*) T. J. Sørensen and B. W. Laursen, *J. Org. Chem.*, 2010, **75**, 6182–6190; (*d*) F. Westerlund, C. B. Hildebrandt, T. J. S. ørensen and B. W. Laursen, *Chem.–Eur. J.*, 2010, **16**, 2992–2996; (*e*) A. Pothukuchy, S. Ellapan, K. R. Gopidasb and M. Salazara, *Bioorg. Med. Chem. Lett.*, 2003, **13**, 1491–1494; (*f*) J. Reynisson, R. Wilbrandt, V. Brinck, B. W. Laursen, K. Nørgaard, N. Harrit and A. M. Brouwer, *Photochem.*

Photobiol. Sci., 2002, **1**, 763–773; (*g*) B. W. Laursen and F. C. Krebs, *Angew. Chem., Int. Ed.*, 2000, **39**, 3432–3434; *Angew. Chem.*, 2000, **112**, 3574–3576.

20 (*a*) DFT calculations on $TOTA^+$ are reported in the ESI,†; (*b*) The AN of **1-BAr$^F_4$** was measured following the Gutmann–Beckett method (see ESI†).

21 (*a*) R. Löw, T. Rusch, T. Moje, F. Röhricht, O. M. Magnussen and R. Herges, *Beilstein J. Org. Chem.*, 2019, **15**, 1815–1821; (*b*) M. Lofthagen, R. Vernonclark and K. K. Baldridge, *J. Org. Chem.*, 1992, **57**, 61–69; (*c*) P. Huszthy, K. Lempert and G. Simig, *J. Chem. Soc., Perkin Trans. 2*, 1985, 1351–1354.

22 T. J. Herrington, A. J. W. Thom, A. J. P. White and A. E. Ashley, *Dalton Trans.*, 2012, **41**, 9019–9022.

23 J.-M. Denis, H. Forintos, H. Szelke, L. Toupet, T.-N. Pham, P.-J. Madecb and A.-C. Gaumont, *Chem. Commun.*, 2003, 54–55.

24 (*a*) H. Clavier and S. P. Nolan, *Chem. Commun.*, 2010, **46**, 841–861; (*b*) C. A. Tolman, *Chem. Rev.*, 1977, **77**, 313–348.

25 L. Rocchigiani, G. Ciancaleoni, C. Zuccaccia and A. Macchioni, *J. Am. Chem. Soc.*, 2014, **136**, 112–115.

26 (*a*) L. Fan, A. R. Jupp and D. W. Stephan, *J. Am. Chem. Soc.*, 2018, **140**, 8119–8123; (*b*) O. J. Metters, S. J. K. Forrest, H. A. Sparkes, I. Manners and D. F. Wass, *J. Am. Chem. Soc.*, 2016, **138**, 1994–2003.

27 ^{19}F–^{1}H HOESY NMR experiments did not reveal the presence of an interaction between $TOTA^+$ and the BAr^F_4 counter ions (Fig. S35 and S43†).

28 (*a*) A. J. V. Marwitz, J. L. Dutton, L. G. Mercier and W. E. Piers, *J. Am. Chem. Soc.*, 2011, **133**, 10026–10029; (*b*) L. C. Brown, J. M. Hogg, M. Gilmore, L. Moura, S. Imberti, S. Gärtner, H. Q. N. Gunaratne, R. J. O'Donnell, N. Artioli, J. D. Holbrey and M. Swadźba-Kwaśny, *Chem. Commun.*, 2018, **54**, 8689–8692.

29 P. Skowronek, J. Ścianowski, A. J. Pacuła and J. Gawroński, *RSC Adv.*, 2015, **5**, 69441–69444.

30 T. C. Johnstone, G. N. J. H. Wee and D. W. Stephan, *Angew. Chem. Int. Ed.*, 2018, **57**, 5881–5884; *Angew. Chem.*, 2008, **130**, 5983–5986.

31 A. M. Chapman, M. F. Haddow and D. F. Wass, *J. Am. Chem. Soc.*, 2011, **133**, 18463–18478.

32 D. H. A. Boom, A. R. Jupp, M. Nieger, A. W. Ehlers and J. C. Slootweg, *Chem.–Eur. J.*, 2019, **25**, 13299–13308.

33 M. J. Sabacky, C. S. Johnson, R. G. Smith, H. S. Gutowsky and J. C. Martin, *J. Am. Chem. Soc.*, 1967, **89**, 2054–2058.

34 E. Müller, A. Moosmayer, A. Rieker and K. Scheffler, *Tetrahedron Lett.*, 1967, **39**, 3877–3880.

35 S. Dileesh and K. R. Gopidas, *Chem. Phys. Lett.*, 2000, **330**, 397–402.

36 Selected review:(*a*) D. Ayan, E. Richards and R. Melen, *Angew. Chem., Int. Ed.*, 2021, **60**, 53–65selected examples:(*b*) Z. Dong, C. Pezzato, A. Sienkiewicz, R. Scopelliti, F. Fadaei-Tirani and K. Severin, *Chem. Sci.*, 2020, **11**, 7615–7618; (*c*) R. J. Andrews and D. W. Stephan, *Chem.–Eur. J.*, 2020, **26**, 7194–7198.

37 (*a*) F. Holtrop, A. R. Jupp, B. J. Kooij, N. P. van Leest, B. de Bruin and J. C. Slootweg, *Angew. Chem., Int. Ed.*, 2020, **59**, 22210–22216; (*b*) A. Merk, H. Großekappenberg, M. Schmidtmann, M.-P. Luecke, C. Lorent, M. Driess, M. Oestreich, H. F. T. Klare and T. Müller, *Angew. Chem., Int. Ed.*, 2018, **57**, 15267–15271.